A Theoretical Study on C_2HXSi Silylenes (X = H, CN, NH_2, and OMe)

M. Z. Kassaee, S. M. Musavi, and M. Ghambarian

Department of Chemistry, Tarbiat Modares University, P.O. Box 14155-4838, Tehran, Iran

Received 25 December 2005; revised 17 April 2006

ABSTRACT: *Relative stabilities and structural characters of 30 silylenic C_2HXSi species (X = H, NH_2, CN, and OMe), with singlet (s) and/or triplet (t) states, are calculated at six levels of theory: HF/6-311++G**, MP3/6-31G*, B1LYP/6-311++G**, B3LYP/6-311++G**, MP2/6-311++G**, and MP4(SDTQ)/6-311++G**. The four possible isomers considered for C_2SiHX are (i) 3-X-1-silacyclopropenylidene (1_{s-X} and 1_{t-X}), (ii) X-vinilydensilylene (2_{s-X} and 2_{t-X}), (iii) ethynyl-X-silylene (3_{s-X} and 3_{t-X}), and (iv) (X-ethynyl)silylene (4_{s-X} and 4_{t-X}). The GIAO–NICS calculations show that singlet cyclic structures, 1_{s-X}, are considerably more aromatic than benzene. Conversely, triplet cyclic C_2HCNSi breaks down through optimization, and transforms into a novel high-spin acyclic carbenosilylene minimum (1_{t-CN}). Singlet 3_{s-NH_2} and triplet 3_{t-NH_2} cross at a divalent angle ($\angle XSiC$) of 152°. This angle narrows to 137° for crossing of singlet 3_{s-CN} and triplet, 3_{t-CN}. The smallest $\angle XSiC$ occurs at 132° for crossing of 3_{s-H} and 3_{t-H}. © 2007 Wiley Periodicals, Inc. Heteroatom Chem 18:283–293, 2007; Published online in Wiley InterScience (www.interscience.wiley.com). DOI 10.1002/hc.20297*

INTRODUCTION

Carbenes and their silylenic analogues are considered as important reactive intermediates [1–12]. Although the ground states of CH_2 and most of its derivatives are a $^3B_1$ triplet (t), the ground state of SiH_2 is a closed shell $^1A_1$ singlet (s) [9–11]. In the case

Correspondence to: M. Z. Kassaee; e-mail: Kassaem@Modares.ac.ir.

of carbenes, Coulomb repulsion between the electrons constrained to the carbon-centered HOMO is large, and some energy must be surmounted to separate the electrons to different molecular orbitals, which are largely compensated by accompanying decrease of electron–electron repulsions. In the case of the heavier low-coordinate species, the energy difference between the similar orbitals is large; furthermore, less energy is gained upon release of the electron–electron repulsion energy. Thus, heavier low-coordinate species favor the closed shell, singlet state [13]. The effect of substituent on the ground state of carbenes and silylenes has been extensively studied, and it has been shown that the most important factor in the stabilization of singlet carbenes is the π-electron donation from the substituent to the divalent atom [14–17]. In contrast, the triplet state can be stabilized by electropositive substituents [18–24]. Regardless of the multiplicity, it is often very difficult to isolate carbenes and/or silylenes. Some small and recently matrix-isolated silylenes are C_2H_2Si [25–27]. These silylenes are among the reactive intermediates that have been of great interest to us [28–32]. Specifically, we have recently reported the ab initio study on singlet–triplet energy separations of C_2HXSi silylenes (X = H, F, Cl, and Br) [31].

In this paper, we examine the electronic effects of amino, cyano, and methoxy groups on the stability order and multiplicities of C_2H_2Si (Fig. 1).

COMPUTATIONAL METHODS

All calculations in this work are performed using the Gaussian 98 program package [33]. The
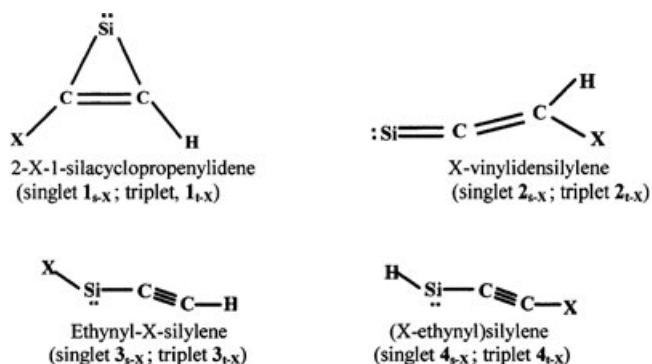
FIGURE 1 The possible structures for singlet(**s**) and triplet(**t**) silylenic C_2HXSi isomers (**1, 2, 3**, and **4**; where X = H, CN, NH_2 and OMe).

structures of all silylenic molecules are fully optimized using standard quantum chemical ab initio and DFT methods. Optimizations are preformed without any symmetrical restrictions. For DFT calculations, the Becke's hybrid one-parameter and three-parameter nonlocal functional were employed, using the LYP correlation with the 6-311++G** basis set [34,35]. For the second-order MØller–Plesset (MP2) method, 6-311++G** basis set is employed, and for the third-order MØller-Plesset (MP3) method, 6-31G* basis set is employed [36,37]. The MP2/6-311++G** optimized geometries are used as input for single-point calculations, at the MP4/6-311++G** [38]. Singlet states are calculated with spin-restricted wave functions, while triplet states are calculated using spin-projected wave functions [39]. The vibrational frequencies and ZPE data

at the HF, B3LYP, and MP2 are scaled by 0.89, 0.98, and 0.92, respectively [40,41]. The NBO population analysis is accomplished at the B3LYP/6-311++G** level [42]. Nucleus independent chemical shift (NICS) values [43] are calculated by the gauge-independent atomic orbital (GIAO) method [44,45] at the B3LYP/6-311++G**. Values of NICS are measured at the ring center, defined as the simple average of Cartesian coordinates for three atoms of three-membered rings, as well as 0.5, 1.0, 1.5, 2.0, 2.5, and 3 Å above the plane of the rings.

RESULTS AND DISCUSSION

In this section, first the results are listed and then they are followed by discussion. The relative energies of 30 possible structures of X-silylenes (C_2HXSi, **1–4**, X = H, NH_2, CN, and OMe) are calculated at HF/6-311++G**, MP3/6-31G*, B1LYP/6-311++G**, B3LYP/6-311++G**, MP2/6-311++G**, and MP4(SDTQ)/6-311++G** levels (Fig. 1, Tables 1–4). We deliberately report the results at several levels of theory in order to offer a forum for a comparison of various levels. It is noteworthy that the same global minima are suggested by all calculation methods for every isomeric series of silylenes **1** through **4**. B3LYP/6-311++G** calculated dipole moments and vibrational zero-point energies (ZPE) are also presented (Tables 1–4). The energy results are dependent on the computational methods employed. Moreover, the energy results obtained at the HF level are different from the results obtained by other calculation methods.

TABLE 1 Relative Energies (kcal/mol), with ZPE Corrections, for Singlet (1_{s-H}, 2_{s-H}, and 3_{s-H}) and Triplet States (1_{t-H}, 2_{t-H}, and 3_{t-H}) of Silylenic C_2H_2Si Calculated at Six Levels of Theory: HF/6-311++G**, MP3/6-31G*, B1LYP/6-311++G**, B3LYP/6-311++G**, MP2/6-311++G**, and MP4(SDTQ)/6-311++G**, Along with Dipole Moments (Debye) and Vibrational Zero-Point Energies (kcal/mol) Calculated via B3LYP/6-311++G**

	Relative Energies (kcal/mol)						Dipole Moments (D)	Vibrational Zero-Point Energies (kcal/mol)
Structure	HF/6-311++G**	MP3/6-31G*[a]	B1LYP/6-311++G**	B3LYP/6-311++G**	MP2/6-311++G**	MP4(SDTQ)/6-311++G**[a]	B3LYP/6-311++G**	B3LYP/6-311++G**
1_{s-H}[b]	0.00	0.00	0.00	0.00	0.00	0.00	0.95	18.50
1_{t-H}	59.85	72.01	70.66	70.69	70.05	71.56	0.81	17.16
2_{s-H}	19.76	18.50	14.75	14.66	20.52	17.03	0.97	17.97
2_{t-H}	24.39	88.77	35.26	35.84	51.39	47.07	1.28	17.04
3_{s-H}	16.26	25.73	17.46	17.80	22.57	20.90	0.89	15.47
3_{t-H}	23.29	51.15	41.35	41.86	48.66	49.22	0.32	15.40

[a]ZPE not included.
[b]The lowest energy minimum sets at 0.00 kcal/mol; total energies (hartrees) for 1_{s-H} at various levels of theory sorted above, respectively: −365.7686985, −366.0681908, −366.8003014, −366.8630339, −366.1172883, and −366.1604181.

TABLE 2 Relative Energies (kcal/mol), with ZPE Corrections, for Singlet (**1$_{s-CN}$**, **2$_{s-CN}$**, **3$_{s-CN}$**, and **4$_{s-CN}$**) and Triplet States (**1$_{t-CN}$**, **2$_{t-CN}$**, **3$_{t-CN}$**, and **4$_{t-CN}$**) of Silylenic C$_2$HCNSi Calculated at Six Levels of Theory: HF/6-311++G**, MP3/6-31G*, B1LYP/6-311++G**, B3LYP/6-311++G**, MP2/6-311++G**, and MP4(SDTQ)/6-311++G**, Along with Dipole Moments (Debye) and Vibrational Zero-Point Energies (kcal/mol) Calculated via B3LYP/6-311++G**

	Relative Energies (kcal/mol)						Dipole Moments (D)	Vibrational Zero-Point Energies (kcal/mol)
Structure	HF/6-311++G**	MP3/6-31G$^{*\,a}$	B1LYP/6-311++G**	B3LYP/6-311++G**	MP2/6-311++G**	MP4(SDTQ)/6-311++G$^{**\,a}$	B3LYP/6-311++G**	B3LYP/6-311++G**
1$_{s-CN}$[b]	0.00	0.00	0.00	0.00	0.00	0.00	3.87	18.19
1$_{t-CN}$[b]	25.46	119.11	45.69	45.91	82.54	74.55	4.52	16.14
2$_{s-CN}$	23.96	21.42	19.23	19.18	23.22	20.09	3.56	17.98
2$_{t-CN}$	26.61	50.31	38.99	39.63	60.00	55.10	4.20	17.23
3$_{s-CN}$	7.35	13.47	9.94	10.54	11.51	10.02	4.00	16.56
3$_{t-CN}$	18.80	48.57	39.21	39.88	49.48	49.29	4.22	16.65
4$_{s-CN}$	20.48	27.77	18.50	18.53	24.12	22.81	3.70	15.37
4$_{t-CN}$	21.66	61.14	40.79	40.99	–	63.13	4.63	15.29

[a]ZPE not included.
[b]The lowest energy minimum sets at 0.00 kcal/mol; total energies (hartrees) for **1$_{s-CN}$** at various levels of theory sorted above, respectively: −457.524831, −458.0720958, −459.0387106, −459.1335881, −458.1580243, and −458.2170544.

Nevertheless, a rather conspicuous consistency appears between different orders of calculated relative energies (Tables 1–4). Spin-contamination is not anticipated to be a problem for the silylenes studied, and their MP4(SDTQ) calculated energies are justified [46,47], because expectation values $\langle S^2 \rangle$ for MP4-calculated triplet states always appear reasonably close to 2.00 (<2.04). On the other hand, B3LYP appears quite reliable for computing of geometrical parameters [29–31]. The NICS values for all singlet cyclic structures are calculated at B3LYP/6-311++G** (Table 5). The selected optimized geometrical parameters are reported at B3LYP/6-311++G** and MP2/6-311++G** levels (Tables 6–9). Nearly similar results are obtained for the geometrical parameters optimized through methods other than B3LYP/6-311++G** and MP2/6-311++G** that are not included in Tables 6–9. Atomic charges and bond orders are significant parameters for our investigation. These quantities are derived from the NBO population analysis [42]. The NBO method is preferred to Mulliken charges,

TABLE 3 Relative Energies (kcal/mol), with ZPE Corrections, for Singlet (**1$_{s-NH_2}$**, **2$_{s-NH_2}$**, **3$_{s-NH_2}$**, and **4$_{s-NH_2}$**) and Triplet States (**3$_{t-NH_2}$** and **4$_{t-NH_2}$**) of Silylenic C$_2$HNH$_2$Si; Calculated at Six Levels of Theory: HF/6-311++G**, MP3/6-31G*, B1LYP/6-311++G**, B3LYP/6-311++G**, MP2/6-311++G**, and MP4(SDTQ)/6-311++G**, Along with Dipole Moments (Debye) and Vibrational Zero-Point Energies (kcal/mol) Calculated via B3LYP/6-311++G**

	Relative Energies (kcal/mol)						Dipole Moments (D)	Vibrational Zero-Point Energies (kcal/mol)
Structure	HF/6-311++G**	MP3/6-31G$^{*\,a}$	B1LYP/6-311++G**	B3LYP/6-311++G**	MP2/6-311++G**	MP4(SDTQ)/6-311++G$^{**\,a}$	B3LYP/6-311++G**	B3LYP/6-311++G**
1$_{s-NH_2}$	11.28	5.11	8.60	7.92	8.21	8.94	2.75	29.65
2$_{s-NH_2}$	29.07	22.24	21.12	20.31	24.68	23.31	3.94	29.91
3$_{s-NH_2}$[b]	0.00	0.00	0.00	0.00	0.00	0.00	1.70	28.38
3$_{t-NH_2}$	27.77	48.37	43.90	44.04	48.15	50.29	1.51	26.68
4$_{s-NH_2}$	30.57	35.61	28.49	28.01	37.37	35.80	4.45	26.24
4$_{t-NH_2}$	42.51	63.04	55.89	55.58	64.62	65.78	3.58	29.65

[a]ZPE not included.
[b]The lowest energy minimum sets at 0.00 kcal/mol; total energies (hartrees) for **3$_{s-NH_2}$** at various levels of theory sorted above, respectively: −420.8491137, −421.2873096, −422.1802271, −422.2675927, −421.377239, and −421.4320371.

TABLE 4 Relative Energies (kcal/mol), with ZPE Corrections, for Singlet ($1_{s\text{-}OMe}$, $2_{s\text{-}OMe}$, $3_{s\text{-}OMe}$, and $4_{s\text{-}OMe}$) and Triplet States ($1_{t\text{-}OMe}$, $2_{t\text{-}OMe}$, and $4_{t\text{-}OMe}$) of Silylenic $C_2HOMeSi$; Calculated at Six Levels of Theory: HF/6-311++G**, MP3/6-31G*, B1LYP/6-311++G**, B3LYP/6-311++G**, MP2/6-311++G**, and MP4(SDTQ)/6-311++G**, Along with Dipole Moments (Debye) and Vibrational Zero-Point Energies (kcal/mol) Calculated via B3LYP/6-311++G**

	Relative Energies (kcal/mol)						Dipole Moments (D)	Vibrational Zero-Point Energies (kcal/mol)
Structure	HF/6-311++G**	MP3/6-31G*[a]	B1LYP/6-311++G**	B3LYP/6-311++G**	MP2/6-311++G**	MP4(SDTQ)/6-311++G**[a]	B3LYP/6-311++G**	B3LYP/6-311++G**
$1_{s\text{-}OMe}$	20.12	12.52	16.83	16.90	15.41	15.69	2.46	39.52
$1_{t\text{-}OMe}$	79.92	86.23	86.46	86.41	86.95	88.55	2.65	38.51
$2_{s\text{-}OMe}$	34.90	25.93	26.31	26.20	27.63	25.67	1.44	39.98
$2_{t\text{-}OMe}$	52.18	103.68	62.37	63.29	75.34	71.29	1.34	38.88
$3_{s\text{-}OMe}$[b]	0.00	0.00	0.00	0.00	0.00	0.00	0.69	38.10
$4_{s\text{-}OMe}$	41.77	45.54	39.81	40.14	46.12	44.78	3.86	36.82
$4_{t\text{-}OMe}$	52.07	71.45	66.06	66.59	72.49	73.80	3.17	36.68

[a]ZPE not included.
[b]The lowest energy minimum sets at 0.00 kcal/mol; total energies (hartrees) for $3_{s\text{-}OMe}$ at various levels of theory sorted above, respectively: −479.717929, −480.2898738, −481.3408093, −481.4536919, −480.4101577, and −480.4798227.

because the former provides an orbital picture that is closer to the classical Lewis structure. The NBO analysis involving atomic charges, bond orders as well as hybridizations of selected bonds are calculated at B3LYP/6-311++G** (Tables 10 and 11). For both singlet and triplet isomers of C_2HXSi, energies of HOMO and LUMO orbitals are obtained by means of NBO analysis. Linear correlations are found between the LUMO–HOMO energy gaps of the singlet silylenes and their corresponding singlet–triplet energy separations, $\Delta E_{s\text{-}t,X}$, calculated at B3LYP/6-311++G** (Fig. 2). The LUMO–HOMO energy gaps of $1_{s\text{-}X}$, $2_{s\text{-}X}$, and $4_{s\text{-}X}$ structures are found to change little as a function of X (Fig. 1). In contrast, LUMO–HOMO energy gaps of $3_{s\text{-}X}$ change drastically as a function of substituents X. The linearity trend is $2_{s\text{-}X}(R^2 = 1.00) > 3_{s\text{-}X}$ $(R^2 = 0.99) >$
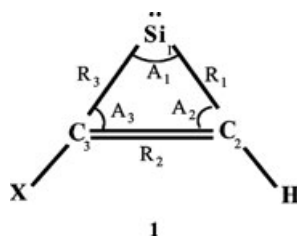
$4_{s\text{-}X}$ $(R^2 = 0.94) > 1_{s\text{-}X}$ $(R^2 = 0.72)$, where R^2 is a correlation coefficient). Slopes may serve as a measure of sensitivity toward substituents. Slopes of linear curves appear negative with the following trend: $4_{s\text{-}X}(m = -2.10) > 3_{s\text{-}X}$ $(m = -1.49) > 2_{s\text{-}X}$ $(m = -1.05) > 1_{s\text{-}X}$ $(m = -0.19)$.

The magnitude of divalent bond angle is one of the most significant parameters that affect $\Delta E_{s\text{-}t,X}$ and/or the ground state multiplicity of silylenes [20]. Bending potential energy curves for acyclic $3_{s\text{-}X}$ and $3_{t\text{-}X}$ species are calculated at B3LYP/6-311++G** (Fig. 3). The divalent angle ∠XSiC, at which singlet $3_{s\text{-}X}$ and triplet $3_{t\text{-}X}$ states cross, appears as a function of X: NH_2 (152°) > CN (137°) > H (132°). This trend follows the electronegativity of the atom directly attached to the divalent atom (Fig. 1). Harmonic vibrational frequencies are calculated for optimized

TABLE 5 The NICS (Total) Values (ppm) at the Ring Centers, NICS(0), and 0.5, 1, 1.5, 2, 2.5, and 3 Å Above the Plane of Rings (NICS(0.5), NICS(1), NICS(1.5), NICS(2), NICS(2.5), and NICS(3), respectively), for Singlet (s) States of $SiC_2H\text{-}X$ ($1_{s\text{-}X}$, X = H, CN, NH_2, and OMe) Silylenes as well as the Cyclopropenyl Cation, Cyclopropenyl Anion, Cyclopropenyl Radical, Cyclopropenylidene (Singlet), and Cyclopropenylidene (Triplet) (Which is Used for Comparison), Calculated at GIAO-B3LYP/6-311++G**// B3LYP/6-311++G** Level

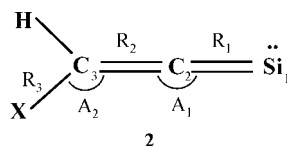| Structure	NICS(0)	NICS(0.5)	NICS(1)	NICS(1.5)	NICS(2)	NICS(2.5)	NICS(3)
$1_{s\text{-}H}$	−14.26	−19.31	−13.89	−7.20	−3.72	−2.14	−1.37
$1_{s\text{-}CN}$	−16.07	−19.70	−13.53	−6.88	−3.51	−2.00	−1.28
$1_{s\text{-}NH_2}$	−21.92	−22.87	−13.79	−6.30	−2.91	−1.55	−0.96
$1_{s\text{-}OMe}$	−19.38	−21.32	−13.36	−6.25	−2.95	−1.59	−0.99
Cyclopropenyl cation	−22.85	−28.50	−14.69	−6.11	−2.89	−1.60	−1.01
Cyclopropenyl anion	4.20	14.99	16.64	9.79	4.95	2.29	0.95
Cyclopropenyl radical	−9.49	−0.51	5.2	3.25	1.49	0.61	0.21
Cyclopropenylidene (singlet)	−16.76	−27.46	−17.07	−7.79	−3.78	−2.09	−1.30
Cyclopropenylidene (triplet)	−36.86	−20.32	−3.07	0.39	0.56	0.35	0.18

TABLE 6   Optimized Geometrical Parameters (Bond Lengths (R) and Bond Angles (A)) Along with Symmetry for Singlet (**s**) and Triplet (**t**) X-silacyclopropenylidene (**1$_{s-x}$** and **1$_{t-x}$**), at Two Levels of Theory: First Line, B3LYP/6-311++G**; Second Line (in Italics), *MP2/6-311++G** for X = H, CN, NH$_2$, and OMe


1

Structure/	Bond Lengths (Å)			Bond Angles (Degrees)		
Symmetry	R_1	R_2	R_3	A_1	A_2	A_3
1$_{s-H}$($C_{2}v$)	1.83	1.34	1.83	42.8	68.6	68.6
	1.83	*1.35*	*1.83*	*43.3*	*68.3*	*68.3*
1$_{s-CN}$(C_S)	1.83	1.35	1.85	42.9	69.2	67.9
	1.84	*1.36*	*1.84*	*43.3*	*68.7*	*68.0*
1$_{s-NH_2}$(C_1)	1.81	1.36	1.85	43.6	69.9	66.4
	1.81	*1.37*	*1.84*	*43.9*	*69.2*	*66.9*
1$_{s-OMe}$(C_S)	1.83	1.35	1.83	43.2	68.4	68.4
	1.84	*1.36*	*1.83*	*43.5*	*67.9*	*68.5*
1$_{t-H}$($C_{2}v$)	1.84	1.35	1.84	43.2	68.4	68.4
	1.83	*1.36*	*1.83*	*43.7*	*68.2*	*68.2*
1$_{t-CN}$[a]	–	–	–	–	–	–
	–	*–*	*–*	*–*	*–*	*–*
1$_{t-OMe}$(C_S)	1.86	1.35	1.83	43.5	67.0	69.4
	1.83	*1.35*	*1.85*	*43.3*	*69.1*	*67.7*

[a]Cyclic triplet structure turns out to be rupture upon optimization.

TABLE 7   Optimized Geometrical Parameters (Bond Lengths (R) and Bond Angles (A)) Along with Symmetry for Singlet (**s**) and Triplet (**t**) X-vinilydenesilylene (**2$_{s-x}$** and **2$_{t-x}$**), at Two Levels of Theory: First Line, B3LYP/6-311++G**; Second Line (in Italics), *MP2/6-311++G** for X = H, CN, NH$_2$, and OMe


2

Structure/	Bond Lengths (Å)			Bond Angles (Degrees)	
Symmetry	R_1	R_2	R_3	A_1	A_2
2$_{s-H}$($C_{2}v$)	1.70	1.32	1.09	179.9	123.4
	1.70	*1.34*	*1.09*	*179.9*	*122.0*
2$_{s-CN}$(C_S)	1.70	1.33	1.43	179.8	123.3
	1.71	*1.34*	*1.43*	*179.8*	*124.8*
2$_{s-NH_2}$(C_S)	1.67	1.35	1.35	178.0	125.9
	1.68	*1.36*	*1.35*	*176.8*	*124.9*
2$_{s-OMe}$(C_S)	1.67	1.34	1.39	175.9	127.6
	1.68	*1.35*	*1.33*	*177.0*	*126.5*
2$_{t-H}$($C_{2}v$)	1.77	1.34	1.41	179.8	123.2
	1.81	*1.30*	*1.09*	*179.1*	*124.7*
2$_{t-CN}$(C_S)	1.79	1.34	1.38	179.2	127.6
	1.83	*1.29*	*1.46*	*179.4*	*121.8*
2$_{t-OMe}$(C_S)	1.79	1.33	1.36	177.0	128.0
	1.82	*1.32*	*1.35*	*177.9*	*127.9*

TABLE 8 Optimized Geometrical Parameters (Bond Lengths (R) and Bond Angles (A)) Along with Symmetry for Singlet (**s**) and Triplet (**t**) Ethynyl-X-silylene (**3$_{s-x}$** and **3$_{t-x}$**), at Two Levels of Theory: First Line, B3LYP/6-311++G**; Second Line (in (Italics), *MP2/6-311++G** for X = H, CN, NH$_2$, and OMe

3
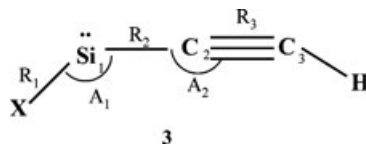
Structure/ Symmetry	Bond Lengths (Å)			Bond Angles (Degrees)	
	R_1	R_2	R_3	A_1	A_2
3$_{s-H}$(C_s)	1.52	1.84	1.22	93.9	171.5
	1.51	*1.84*	*1.23*	*94.3*	*168.8*
3$_{s-CN}$(C_s)	1.89	1.84	1.22	95.8	169.5
	1.88	*1.84*	*1.23*	*95.3*	*169.1*
3$_{s-NH_2}$(C_s)	1.72	1.87	1.21	97.5	169.3
	1.72	*1.87*	*1.23*	*96.6*	*169.8*
3$_{s-OMe}$(C_1)	1.67	1.86	1.21	97.7	167.7
	1.66	*1.85*	*1.23*	*97.3*	*167.2*
3$_{t-H}$(C_s)	1.48	1.78	1.22	118.6	173.9
	1.47	*1.83*	*1.19*	*116.8*	*176.6*
3$_{t-CN}$(C_s)	1.81	1.77	1.22	119.1	173.0
	1.86	*1.82*	*1.19*	*113.9*	*174.7*
3$_{t-NH_2}$(C_s)	1.74	1.79	1.22	118.8	173.6
	1.72	*1.84*	*1.19*	*117.6*	*176.4*

structures at HF, DFT, and MP2 levels. This not only assists in the estimation of the zero-point vibrational energy correction but also allows assessing the nature of the stationary points on their potential energy surfaces. Among 30 structures, force constant calculations show only three triplets **1$_{t-NH_2}$**, **2$_{t-NH_2}$**, and **3$_{t-OMe}$**, which exist as transition states, having one imaginary frequency. Computed harmonic frequencies are not provided for the sake of brevity.

TABLE 9 Optimized Geometrical Parameters (Bond Lengths (R) and Bond Angles (A)) Along with Symmetry for Singlet (**s**) and Triplet (**t**) (X-e thynyl)silylene (**4$_{s-x}$** and **4$_{t-x}$**), at Two Levels of Theory: First Line, B3LYP/6-311++G**; Second Line (in Italics), *MP2/6-311++G** for X = H, CN, NH$_2$, and OMe

4
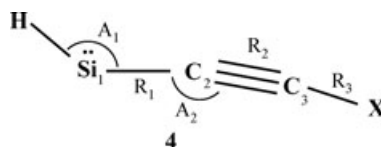
Structure/ Symmetry	Bond Lengths (Å)			Bond Angles (Degrees)	
	R_1	R_2	R_3	A_1	A_2
4$_{s-CN}$(C_s)	1.84	1.22	1.36	92.8	171.2
	1.85	*1.23*	*1.37*	*93.4*	*167.7*
4$_{s-NH_2}$(C_1)	1.80	1.23	1.31	97.0	172.0
	1.81	*1.24*	*1.33*	*94.5*	*168.6*
4$_{s-OMe}$(C_s)	1.81	1.22	1.28	94.5	170.9
	1.82	*1.24*	*1.29*	*94.7*	*167.5*
4$_{t-CN}$(C_s)	1.77	1.23	1.36	118.5	172.9
	1.85	*1.17*	*1.42*	*115.2*	*175.9*
4$_{t-NH_2}$(C_s)	1.77	1.23	1.32	117.7	167.1
	1.80	*1.21*	*1.34*	*118.5*	*177.0*
4$_{t-OMe}$(C_1)	1.77	1.23	1.29	118.3	170.4
	1.80	*1.21*	*1.29*	*118.2*	*177.2*

TABLE 10 The NBO Analysis Including Atomic Charges and Bond Orders of C$_2$HXSi (X = H, CN, NH$_2$, and OMe) Silylenes **1–4** Calculated at B3LYP/6-311++G**

Structure	Species	Atomic Charge					Bond Order				
		Si	C$_2$	C$_3$	H	X	Si—C$_2$	Si—C$_3$	C$_2$—C$_3$	C$_3$—H	C$_2$—X
1	**1$_{s-H}$**	0.77	−0.59	−0.59	0.21	0.21	0.83	0.83	2.03	1.00	1.00
	1$_{t-H}$	−0.50	−0.36	−0.36	0.11	0.11	−	−	−	−	−
	1$_{s-CN}$	0.88	−0.54	−0.53	0.22	0.24	0.79	0.76	1.95	0.99	1.19
	1$_{t-CN}$	0.71	−0.83	−0.01	0.25	0.12	1.12	0.30	1.90	0.95	1.54
	1$_{s-NH_2}$	0.72	−0.71	−0.20	0.20	−0.78	0.89	0.78	1.90	1.01	1.23
	1$_{s-OMe}$	0.77	−0.71	−0.07	0.21	−0.53	−	−	−	−	−
	1$_{t-OMe}$	0.63	−0.67	0.00	0.21	−0.52	−	−	−	−	−
							Si—C$_2$	C$_2$—C$_3$	C$_3$—H	C$_3$—X	
2	**2$_{s-H}$**	0.77	−0.87	−0.27	0.19	0.19	1.49	1.95	0.98	0.98	
	2$_{t-H}$	0.54	−0.47	−0.53	0.23	0.23	1.34	1.99	0.97	0.97	
	2$_{s-CN}$	0.85	−0.82	−0.24	0.23	0.25	1.42	1.88	0.95	1.10	
	2$_{t-CN}$	−0.06	−0.60	−0.37	0.11	0.14	1.41	1.75	0.94	1.17	
	2$_{s-NH_2}$	0.72	−1.04	0.10	0.18	−0.74	1.51	1.77	0.94	1.22	
	2$_{s-OMe}$	0.79	−1.08	0.26	0.18	−0.51	−	−	−	−	
	2$_{t-OMe}$	−0.21	−0.64	−0.10	0.09	−0.30	−	−	−	−	
							Si—C$_2$	C$_2$—C$_3$	C$_3$—H	Si—X	
3	**3$_{s-H}$**	0.78	−0.61	−0.14	0.22	−0.27	0.72	2.79	1.00	0.70	
	3$_{t-H}$	−0.49	−0.25	−0.25	0.12	−0.13	0.99	2.78	1.01	0.91	
	3$_{s-CN}$	0.99	−0.61	−0.09	0.23	−0.24	−	−	−	−	
	3$_{t-CN}$	−0.30	−0.27	−0.20	0.12	−0.10	0.93	2.78	1.00	0.87	
	3$_{s-NH_2}$	1.00	−0.57	−0.18	0.22	−1.25	0.63	2.82	1.01	0.83	
	3$_{t-NH_2}$	−0.28	−0.29	−0.22	0.11	−0.70	0.96	2.80	1.01	0.92	
	3$_{s-OMe}$	1.10	−0.59	−0.15	0.22	−0.89	0.63	2.81	1.00	0.75	
							Si—C$_2$	C$_2$—C$_3$	C$_3$—X	Si—H	
4	**4$_{s-CN}$**	0.82	−0.45	−0.09	−0.25	0.21	0.71	2.63	1.22	0.69	
	4$_{t-CN}$	−0.41	−0.18	−0.21	−0.12	0.14	1.04	2.58	1.26	0.89	
	4$_{s-NH_2}$	0.68	−0.66	0.21	−0.25	−0.77	0.80	2.52	1.25	0.69	
	4$_{t-NH_2}$	0.62	−0.68	0.22	−0.17	−0.79	1.05	2.53	1.24	0.90	
	4$_{s-OMe}$	0.73	−0.73	0.39	−0.27	−0.49	0.75	0.75	1.06	0.69	
	4$_{t-OMe}$	−0.50	−0.32	0.04	−0.13	−0.27	0.69	2.56	1.06	0.91	

TABLE 11 The NBO Calculated Hybridizations for Cyclic **1$_{s-X}$** and **1$_{t-X}$** and Acyclic **3$_{s-X}$** and **3$_{t-X}$** Silylenes (X = H, CN, NH$_2$, and OMe)

Structure	Bond		Structure	Bond	
	$\sigma_{Si—C_2}$	$\sigma_{Si—C_3}$		$\sigma_{Si—C}$	$\sigma_{Si—X}$
1$_{s-H}$	s^{1}p$^{9.60}$d$^{0.09}$	s^{1}p$^{9.60}$d$^{0.09}$	**3$_{s-H}$**	s^{1}p$^{5.91}$d$^{0.09}$	s^{1}p$^{7.93}$d$^{0.08}$
1$_{t-H}$	s^{1}p$^{7.66}$d$^{0.06}$	s^{1}p$^{7.66}$d$^{0.06}$	**3$_{t-H}$**	s^{1}p$^{4.70}$d$^{0.03}$	s^{1}p$^{3.75}$d$^{0.04}$
1$_{s-CN}$	s^{1}p$^{9.93}$d$^{0.10}$	s^{1}p$^{10.57}$d$^{0.11}$	**3$_{s-CN}$**	s^{1}p$^{5.97}$d$^{0.09}$	s^{1}p$^{7.87}$d$^{0.12}$
1$_{t-CN}$	s^{1}p$^{7.45}$d$^{0.09}$	−	**3$_{t-CN}$**	s^{1}p$^{3.52}$d$^{0.03}$	s^{1}p$^{4.49}$d$^{0.05}$
1$_{s-NH_2}$	s^{1}p$^{7.97}$d$^{0.07}$	s^{1}p$^{10.63}$d$^{0.10}$	**3$_{s-NH_2}$**	s^{1}p$^{6.13}$d$^{0.09}$	s^{1}p$^{5.97}$d$^{0.11}$
1$_{t-NH_2}$	s^{1}p$^{9.27}$d$^{0.10}$	−	**3$_{t-NH_2}$**	s^{1}p$^{4.20}$d$^{0.05}$	s^{1}p$^{4.74}$d$^{0.07}$
1$_{s-OMe}$	s^{1}p$^{8.68}$d$^{0.08}$	s^{1}p$^{9.75}$d$^{0.10}$	**3$_{s-OMe}$**	s^{1}p$^{6.21}$d$^{0.11}$	s^{1}p$^{7.72}$d$^{0.19}$
1$_{t-OMe}$	s^{1}p$^{8.19}$d$^{0.07}$	s^{1}p$^{7.43}$d$^{0.07}$	**3$_{t-OMe}$**	s^{1}p$^{3.52}$d$^{0.04}$	s^{1}p$^{6.12}$d$^{0.14}$

Relative Stability

All singlet species (**1$_{s-X}$**, **2$_{s-X}$**, **3$_{s-X}$**, and **4$_{s-X}$**) appear to be more stable than their corresponding triplets (**1$_{t-X}$**, **2$_{t-X}$**, **3$_{t-X}$**, and **4$_{t-X}$**) (Tables 1–4). The intrinsic tendency of silylenes for singlet ground states is a good reason to justify this phenomenon in agreement with their halogenated analogues [31]. Nevertheless, singlet–triplet cross over diagrams (Fig. 3) may help in designing of new acyclic triplet state silylenes in the future. The relative stability of C$_2$H$_2$Si isomers (X = H), calculated at MP4(SDTQ)/6-311++G**, is **1$_{s-H}$** (0.00 kcal/mol) > **2$_{s-H}$** (17.03 kcal/mol) > **3$_{s-H}$** (20.90 kcal/mol) > **2$_{t-H}$** (47.07 kcal/mol) > **3$_{t-H}$** (49.22 kcal/mol) > **1$_{t-H}$** (71.56 kcal/mol) (Table 1). The structure of the lowest
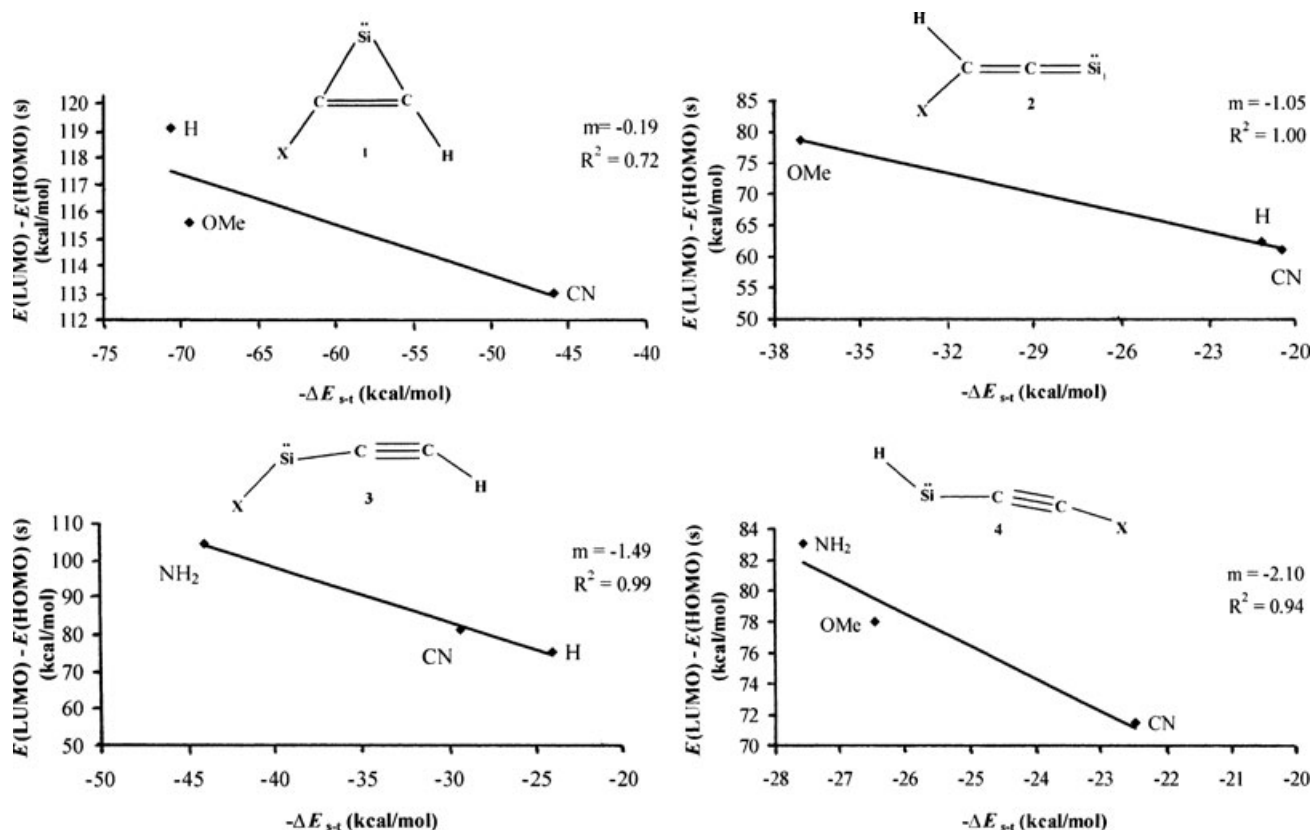
FIGURE 2 Correlations between the LUMO–HOMO energy gaps (kcal/mol) of the singlet (**s**) C_2HXSi silylenes (**1–4**), and their corresponding singlet–triplet energy separations, $\Delta E_{s-t,X}$ (kcal/mol), for X = H, CN, NH_2, and OMe calculated at B3LYP/6-311++G** level of theory (R^2 = correlation coefficient).
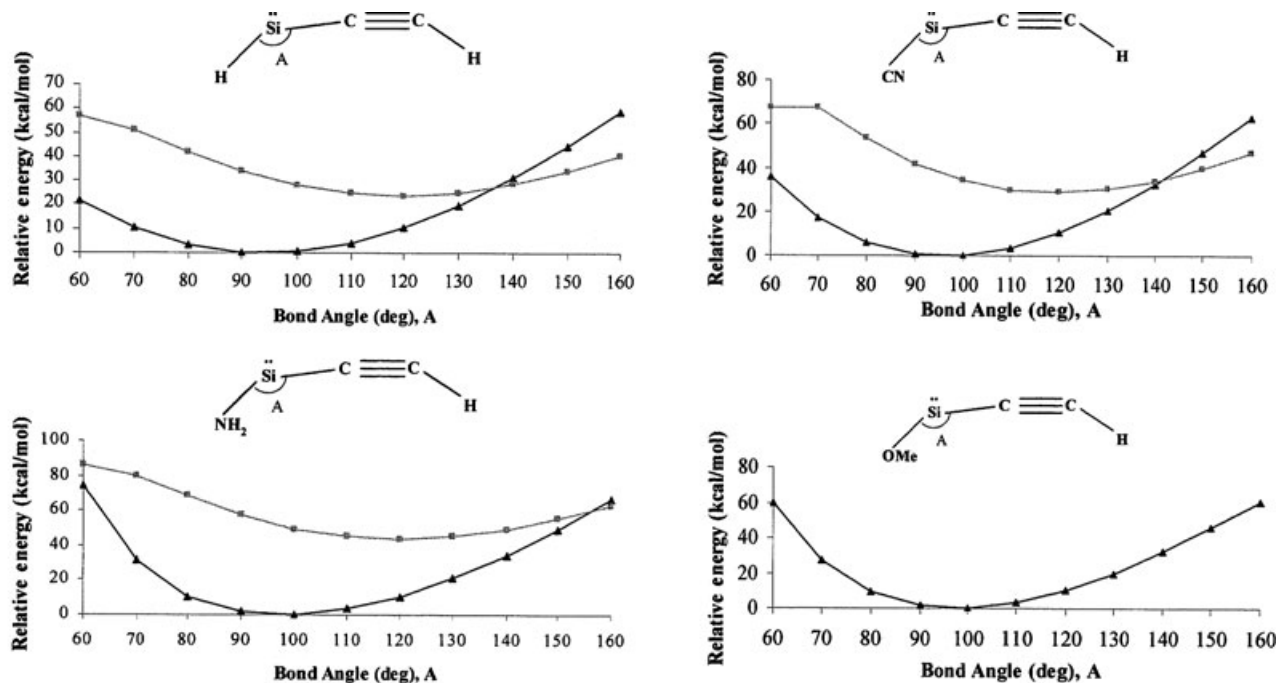

FIGURE 3 Relative energies (kcal/mol) as a function of the divalent bond angle $\angle$XSiC (degrees) (bending potential energy curves) of the singlet (▲) and triplet (■) states of ethyny-X-silylene, 3_{s-x} and 3_{t-x} species, where X = H, CN, NH_2, and OMe (3_{t-OMe} is not a real isomer).

energy (global minimum) among the C$_2$H$_2$Si series appears as a singlet silacyclopropenylidene, **1$_{s-H}$**; it is compatible with the results of Gordon et al. [48]. To justify the above trend, one may point to the aromatic character of **1$_{s-H}$**, caused by incorporating a σ^2 silylenic center within its continuously conjugated three-member ring. The calculated NICS indices [43] are based on the "absolute magnetic shielding," taken at the center of a ring compound, where the full effect of the induced ring current should be observed. Also, NICS(1) (i.e., at points 1 Å above the ring center) was recommended to be a better measure of the π electron delocalization, compared to NICS(0) (i.e., at the ring center) [49]. The calculated NICS indices with negative values are aromatic, and those with positive values are antiaromatic. Our calculated NICS values indicate that all singlet cyclic silylenes, **1$_{s-X}$**, are considerably aromatic with large negative NICS values (Table 5). Moreover, the predicted aromatic characters of **1$_{s-X}$** rings are less than those of analogues singlet cyclopropenylidene (NICS(1) = −17.07 ppm) and cyclopropenyl cation (NICS(1) = −14.69 ppm), but higher than those of benzene ring (NICS(1) = −10.6 ppm) [49,50]. Substituents (X) employed appear to have negligible effects on the aromaticity of singlet silylenes (Table 5). **2$_{s-H}$** is less stable than **1$_{s-H}$**, due to the aromaticity of the latter. The stabilizing effect of an additional Si—C bond in **2$_{s-H}$**, as a replacement for Si—H bond in **3$_{s-H}$**, makes the former more stable than the latter. **2$_{t-H}$** is the most stable triplet isomer among C$_2$H$_2$Si silylenes, which is obviously less stable than the singlet silylene **3$_{s-H}$**. An allylic resonance hybrid contributor justifies higher stability of **2$_{t-H}$** over **3$_{t-H}$**. A less significant vinylic resonance hybrid contributor indicates lower resonance role in stabilizing **3$_{t-H}$** compared to **2$_{t-H}$**. Finally, because of the enormous angle strains, cyclic **1$_{t-H}$** turns out to be the least stable isomer among the silylenic C$_2$H$_2$Si series.

The order of relative stability calculated at MP4(SDTQ)/6-311++G** for C$_2$HCNSi silylenes is **1$_{s-CN}$** (0.00 kcal/mol) > **3$_{s-CN}$** (10.02 kcal/mol) > **2$_{s-CN}$** (20.09 kcal/mol) > **4$_{s-CN}$** (22.81 kcal/mol) > **3$_{t-CN}$** (49.29 kcal/mol) > **2$_{t-CN}$** (55.10 kcal/mol) > **4$_{t-CN}$** (63.13 kcal/mol) > **1$_{t-CN}$** (74.55 kcal/mol) (Table 2). The range of energy differences for C$_2$HCNSi isomers is similar to that of C$_2$H$_2$Si. This is possibly because of the stabilizing effect of cyano group (CN) for both singlet and triplet states, resulting from the high electron withdrawing and/or π-acceptor ability of CN. Same justifications for the relative stability of C$_2$H$_2$Si can be employed to the remaining C$_2$HCNSi isomers.

Recalling the transitory states of triplets **1$_{t-NH_2}$** and **2$_{t-NH_2}$**, the order of relative stability of the remaining isomers (minima) in the C$_2$HNH$_2$Si series, calculated at MP4 (SDTQ)/6-311++G**, is **3$_{s-NH_2}$** (0.00 kcal/mol) > **1$_{s-NH_2}$** (8.94 kcal/mol) > **2$_{s-NH_2}$** (23.31 kcal/mol) > **4$_{s-NH_2}$** (35.80 kcal/mol) > **3$_{t-NH_2}$** (50.29 kcal/mol) > **4$_{t-NH_2}$** (65.78 kcal/mol) (Table 3). In contrast to the above C$_2$H$_2$Si and/or C$_2$HCNSi, in the case of C$_2$HNH$_2$Si structures, the NH$_2$ group (directly attached to the silylenic center) strongly stabilizes the singlet state. It switches the global minimum to singlet acylic **3$_{s-NH_2}$**, instead of singlet aromatic **1$_{s-NH_2}$** (Table 5).

To discuss the C$_2$HOMeSi series, recalling that **3$_{t-OMe}$** is a transition state, the order of relative stability calculated at MP4(SDTQ)/6-311++G** is **3$_{s-OMe}$** (0.00 kcal/mol) > **1$_{s-OMe}$** (15.69 kcal/mol) > **2$_{s-OMe}$** (25.67 kcal/mol) > **4$_{s-OMe}$** (44.78 kcal/mol) > **2$_{t-OMe}$** (71.29 kcal/mol) > **4$_{t-OMe}$** (73.80 kcal/mol) > **1$_{t-OMe}$** (88.55 kcal/mol) (Table 4). This is nearly the same trend found for C$_2$HNH$_2$Si, but with a wide range of energy differences between the isomers involved. Hence, a methoxy group has a higher stabilizing effect on the divalent center than an amino group. One may justify this finding on the basis of the higher electronegativity of oxygen than nitrogen [31]. Again, the global minimum for the set of C$_2$HOMeSi silylenes, offered by all calculation methods, appears to be a singlet acylic **3$_{s-OMe}$**.

Geometries, Dipole Moments, and Atomic Charges

All optimizations are performed without any imposed constraints. Owing to the enormous angle strain in the three-member ring, Si—C$_3$ bonds of cyclic triplet **1$_{t-NH_2}$** and **1$_{t-CN}$** cleave to form an acyclic carbeno-silylene structure (Table 6). In general, geometrical parameters of all silylenes studied change little as a function of substituents X (Tables 6–9). Singlet **1$_{s-H}$** has a planar structure with C_{2v} symmetry, and when H is replaced with CN and/or OMe, the planarity is conserved. In contrast, **1$_{s-NH_2}$** has an asymmetric structure with C_1 point group. All **2$_{s-X}$** and **2$_{t-X}$** structures are also planar with at least C_s point group (Table 7). Likewise, **3$_{s-X}$** and **3$_{t-X}$** structures are planar with C_s point group. An exception is **3$_{s-OMe}$**, which has C_1 symmetry (Table 8). Finally, most **4$_{s-X}$** and **4$_{t-X}$** structures are planar with C_s symmetry, except **4$_{s-NH_2}$** and **4$_{t-OMe}$** that have C_1 symmetry (Table 9). Interestingly, cumulenic moiety C=C=Si in **2$_{s-X}$** and **2$_{t-X}$** has nearly a linear arrangement.

In the acyclic structures **3$_{s-X}$** and **3$_{t-X}$**, the replacement of H for X lengthens Si—C$_2$ bond, as well as rather shortens the C$_2$—C$_3$ bond possibly because of the stabilization effect of divalent center by substituents X in preference to the C$_2$—C$_3$ triple

bond (Table 8). A divalent bond angle $\angle A_1$ in singlet 3_{s-X} species is significantly smaller than that of triplet state 3_{t-X}, in agreement with many acyclic carbenes and silylenes [31]. This finding is justified on the basis of electronic structures and hybridizations of atoms attached to the divalent centers. For instance, strictly localized natural bond orbitals (NBO) of the σ molecular orbitals show higher p characters for bonds connected to the divalent centers of singlet structures 3_{s-X} compared to their corresponding triplets 3_{t-X} (Table 11). Moreover, no silicon d orbital valence participation is found for the scrutinized silylenes (Table 11).

The order of dipole moments for C_2H_2Si isomers is $2_{t-H} > 2_{s-H} > 1_{s-H} > 3_{s-H} > 1_{t-H} > 3_{t-H}$ (Table 1), while the order of dipole moments for C_2HCNSi isomers is $4_{t-CN} > 1_{t-CN} > 3_{t-CN} > 2_{t-CN} > 3_{s-CN} > 1_{s-CN} > 4_{s-CN} > 2_{s-CN}$ (Table 2). C_2HCNSi isomers with X = CN have relatively high dipole moments. Moreover, all triplet states with a C_2HCNSi formula have higher dipole moments than their corresponding singlet states. Likewise, the trend of dipole moments for C_2HNH_2Si isomers is $4_{s-NH_2} > 2_{s-NH_2} > 4_{t-NH_2} > 1_{s-NH_2} > 3_{s-NH_2} > 3_{t-NH_2}$ (Table 3). Finally, the trend of dipole moments for $C_2HOMeSi$ isomers is $4_{s-OMe} > 4_{t-OMe} > 1_{t-OMe} > 1_{s-OMe} > 2_{s-OMe} > 2_{t-OMe} > 3_{s-OMe}$ (Table 4). The structure of the highest dipole moments among **1**–**4** appears to be (X-ethynyl)silylene **4**.

The NBO results reveal two major points. First, optimization of cyclic structure 1_{t-CN} resulted in the cleavage of its Si—C_3 bond, reducing its bond order to 0.3 (Table 10). Consequently, 1_{t-CN} transforms into an acyclic carebeno-silylene structure with no negative force constant. This is mostly due to the electron deficiency of the three-member ring induced by a rather strong electron-withdrawing group, CN. In this work, it is interesting to come across a fairly stable carbeno-silylene structure, because the reported research activities on polydivalent species including dicarbenes, dinitrenes, and carbeno-nitrenes have mainly focused on systems with o-, m-, and p-phenylene bridges [51–53]. Second, the silylenic divalent centers of all singlet species have positive charges (Table 10). This is in contrast to the triplet species, where their silylenic divalent centers mostly possess negative charges.

CONCLUSION

Relative stability as well as the singlet–triplet energy separation ($\Delta E_{s-t,X}$) of several new silylenic reactive intermediates C_2HXSi are compared and contrasted at six ab initio and DFT levels of theory (where X is H, CN, NH_2, and OMe). Four possible structures are anticipated for each singlet (**s**) and/or triplet (**t**) silylenes, C_2HXSi, including 3-X-1-silacyclopropenylidene (**1**), X-vinilydensilylene (**2**), ethynyl-X-silylene (**3**), and (X-ethynyl)silylene (**4**). All singlet silylenes are found to be more stable than their corresponding triplet states. For the six isomers with X = H, the stability order is $1_{s-H} > 2_{s-H} > 3_{s-H} > 2_{t-H} > 3_{t-H} > 1_{t-H}$. Likewise, the stability order of isomers with X = CN is $1_{s-CN} > 3_{s-CN} > 2_{s-CN} > 4_{s-CN} > 3_{t-CN} > 2_{t-CN} > 4_{t-CN} > 1_{t-CN}$. The stability order of isomers with X = NH_2 is $3_{s-NH_2} > 1_{s-NH_2} > 2_{s-NH_2} > 4_{s-NH_2} > 3_{t-NH_2} > 4_{t-NH_2}$. Finally, the order of stability of $C_2SiHOMe$ isomers is $3_{s-OMe} > 1_{s-OMe} > 2_{s-OMe} > 4_{s-OMe} > 2_{t-OMe} > 4_{t-OMe} > 1_{t-OMe}$. The aromaticity of singlet cyclic structures, 1_{s-X}, is measured by GIAO–NICS calculations. Bending potential energy curves are calculated for acyclic silylenes 3_{s-X} and 3_{t-X}, where the cross points of singlet and triplet states are shown. A rather stable carbeno-silylene structure is observed as a minimum on the potential energy surface of C_2HCNSi. Linear correlations are found between the LUMO–HOMO energy gaps of the singlet C_2HXSi silylenes and their corresponding $\Delta E_{s-t,X}$, calculated at B3LYP/6-311++G**. Both electronegativity as well as resonance effects of substituents are important in the stabilization of silylenes. A conspicuous consistency is observed among the trends of relative energies, calculated at various levels that were employed.

REFERENCES

[1] Yamaguchi, Y.; Sherrill, C. D.; Schaefer, H. F., III. J Phys Chem 1996, 100, 7911.
[2] Sherrill, C. D.; Huis, T. J. V.; Yamaguchi, Y.; Schaefer, H. F., III. J Mol Struct (Theochem) 1997, 400, 39.
[3] Sherrill, C. D.; Leininger, M. L.; Huis, T. J. V.; Schaefer, H. F., III. J Chem Phys 1998, 108, 1040.
[4] Garcya, V. M.; Castell, O.; Reguero, M.; Caballol, R. Mol Phys 1996, 87, 1395.
[5] Das, D.; Whittenburg, S. L. J Mol Struct (Theochem) 1999, 492, 175.
[6] Schwartz, M.; Marshall, P. J Phys Chem A 1999, 103, 7900.
[7] Sendt, K.; Bacskay, G. B. J Chem Phys 2000, 112, 2227.
[8] Schwartz, R. L.; Davico, G. E.; Ramond, T. M.; Lineberger, W. C. J Phys Chem A 1999, 103, 8213.

[9] Barden, C. J.; Schaefer, H. F., III. J Chem Phys 2000, 112, 6515.

[10] Lee, E. P. F.; Dyke, J. M.; Wright, T. G. Chem Phys Lett 2000, 326, 143.

[11] Bruce, M. Chem Rev 1991, 91, 197.

[12] Hargittai, M.; Schultz, G.; Schwerdtfeger, P.; Seth, M. Struct Chem 2001, 12, 377.

[13] Rauk, A. Orbital Interaction Theory of Organic Chemistry; Wiley: New York, 2001; Ch. 7.

[14] Luke, B. T.; Pople, J. A.; Krogh-Jespersen, M. B.; Apeloig, Y.; Karni, M.; Chandrasekhar, J.; von Ragué Schleyer, P. J Am Chem Soc 1986, 108, 270.

[15] Nyulaszi, L.; Belghazi, A.; Kis Szetsi, S.; Veszpremi, T.; Heinicke, J. J Mol Struct (Theochem) 1994, 313, 73.

[16] Gordon, M. S.; Bartol, D. J Am Chem Soc 1987, 109, 5948.

[17] Shin, S. K.; Goddard, W. A., III; Beauchamp, J. L. J Phys Chem 1990, 94, 6963.

[18] Arduengo, A. J., III. Acc Chem Res 1999, 32, 913.

[19] Bourissou, D.; Guerret, O.; Gabbay, F. P.; Bertrand, G. Chem Rev 2000, 100, 39.

[20] Gaspar, P. P.; Xiao, M.; Pae, D. H.; Berger, D. J.; Haile, T.; Chen, T.; Lei, D.; Winchester, W. R.; Jiang, P. J Organomet Chem 2002, 646, 68.

[21] Jiang, P.; Gaspar, P. P. J Am Chem Soc 2001, 123, 8622.

[22] Yoshida, M.; Tamaoki, N. Organometallics 2002, 21, 2587.

[23] Holthause, M. C.; Koch, W.; Apeloig, Y. J Am Chem Soc 1999, 121, 2623.

[24] Sekiguchi, A.; Tanaka, T.; Ichinohe, M.; Akiyama, K.; Tero-Kubota, S. J Am Chem Soc 2003, 125, 4962.

[25] Maier, G.; Reisenauer, H. P.; Egenolf, H.; Glatthaar, J. Eur J Org Chem 1998, 1307.

[26] Maier, G.; Reisenauer, H. P.; Egenolf, H.; Meudt, A. Eur J Org Chem 1998, 1313.

[27] Maier, G.; Reisenauer, H. P.; Schwab, W.; Carsky, P.; Hess, B. A.; Schaad, L. J. J Am Soc 1987, 109, 5183.

[28] Kassaee, M. Z.; Ghambarian, M.; Musavi, S. M. J Organomet Chem 2005, 690, 4692.

[29] Kassaee, M. Z.; Musavi, S. M.; Ghambarian, M.; Buazar, F. J Mol Struct (Theochem) 2005, 726, 171.

[30] Kassaee, M. Z.; Musavi, S. M.; Hamadi, H.; Ghambarian, M.; Hosseini, S. E. J Mol Struct (Theochem) 2005, 730, 33.

[31] Kassaee, M. Z.; Musavi, S. M.; Buazar, F.; Ghambarian, M. J Mol Struct (Theochem) 2005, 722, 151.

[32] Kassaee, M. Z.; Musavi, S. M.; Buazar, F. J Mol Struct (Theochem) 2005, 728, 15.

[33] Frisch, M. J.; Trucks, G. W.; Schlegel, H. B.; Scuseria, G. E.; Robb, M. A.; Cheeseman, J. R.; Zakrzewski V. G., Jr.; Montgomery, J. A.; Stratmann, R. E.; Burant, J. C.; Dapprich, S.; Millan, J. M.; Daniels, A. D.; Kudin, K. N.; Strain, M. C.; Farkas, O.; Tomasi, J.; Barone, V.; Cossi, M.; Cammi, R.; Mennucci, B.; Pomelly, C.; Adamo, C.; Clifford, S.; Ochterski, J.; Petersson, G. A.; Ayala, P. Y.; Cui, Q.; Morokuma, K.; Malick, D. K.; Rabuck, A. D.; Raghavachari, K.; Foresman, J. B.; Cioslowski, J.; Ortiz, J. V.; Baboul, A. G.; Stefanov, B. B.; Liu, G.; Liashenko, A.; Piskorz, P.; Komaromi, I.; Gomperts, R.; Martin, R. L.; Fox, D. J.; Keith, T.; Al-Laham, M. A.; Peng, C. Y.; Nanayakkara, A.; Gonzalez, C.; Challacombe, M.; Gill, P. M. W.; Johnson, B.; Chen, W.; Wong, M. W.; Andres, J. L.; Gonzalez, C.; Head-Gordon, M.; Replogle, E. S.; Pople, J. A. Gaussian Inc., Revision A.7, Pittsburgh, PA, 1998.

[34] Becke, A. D. J Chem Phys 1996, 104, 1040.

[35] Adamo, C.; Barone, V. Chem Phys Lett 1997, 274, 242.

[36] Saebo, S.; Almlof, J. Chem Phys Lett 1989, 154, 83.

[37] Pople, J. A.; Binkley, J. S.; Seeger, R. Int J Quant Chem Symp 1976, 10, 1.

[38] Pople, J. A.; Head-Gordon, M.; Raghavachari, K. J Chem Phys 1987, 87, 5968.

[39] Schlegel, H. B. J Phys Chem 1988, 92, 3075.

[40] Hout, R. F.; Levi, B. A.; Heher, W. J. J Comput Chem 1985, 82, 234.

[41] Defrees, D. J.; McLean, A. D. J Chem Phys 1985, 82, 333.

[42] Carpenter, J. E.; Weinhold, F. J Mol Struct (Theochem) 1988, 41, 169.

[43] Schleyer, P. v. R.; Maerker, C.; Dransfeld, A.; Jiao, H.; Hommes, N. J. R. v. E. J Am Chem Soc 1996, 118, 6317.

[44] Chesnut, D. B., Moore, K. D. J Comput Chem 1985, 10, 648.

[45] Wolinski, K.; Hinton, J. F.; Pulay, P. J Am Chem Soc 1990, 112, 8251.

[46] Aoki, K.; Ikuta, S.; Murakami, A. J Mol Struct (Theochem) 1996, 365, 103.

[47] Barrientos, C.; Cimas, A.; Largo, A. J Phys Chem A 2001, 105, 6724.

[48] Schriver, G. W.; Fink, M. J.; Gordon, M. S. Organometallics 1987, 6, 1977.

[49] Schleyer, P. v. R.; Manoharan, M.; Wang, Z. X.; Kiran, B.; Jiao, H.; Puchta, R.; Hommes, N. J. R. v. E. Org Lett 2001, 3, 2465.

[50] Glukhovtsev, M. N.; Sergei, L.; Addy, P. J Phys Chem 1996, 100, 17801.

[51] Harder, T.; Bendig, J.; Scholz, G.; Stosser, R. J Am Chem Soc 1996, 118, 2497.

[52] Nimura, S.; Kikuchi, O.; Ohana, T.; Yabe, A.; Kaise, M. Chem Lett 1996, 125.

[53] Nicolaides, A.; Nakayama, T.; Yamazaki, K.; Tomioka, H.; Koseki, S.; Stracener, L. L.; McMahon, R. J. J Am Chem Soc 1999, 121, 1056.